New & Forthcoming Titles | The International Journal of Advanced Manufacturing Technology-incl. option to publish open access (Editorial Board)

Springer   www.springer.com
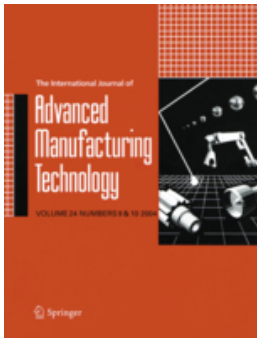
New & Forthcoming Titles   Home   >   New & Forthcoming Titles

The International Journal of Advanced Manufacturing Technology

ISSN: 0268-3768 (print version)
ISSN: 1433-3015 (electronic version)

Journal no. 170

Read Online

125,21 €   Personal Rate e-only

Get Subscription

Online subscription, valid from January through December of current calendar year

Immediate access to this year's issues via SpringerLink

6 Volume(-s) with 72 issue(-s) per annual subscription

Automatic annual renewal

More information: >> FAQs // >> Policy

ABOUT THIS JOURNAL   EDITORIAL BOARD   B. JOHN DAVIES BEST PAPER PRIZE   ETHICS & DISCLOSURE

Editor for India

M. S. Shunmugam
Department of Mechanical Engineering
Indian Institute of Technology Madras
Chennai 600 036, India
e-mail: shun@iitm.ac.in

Editor for the Middle East

Erhan Budak
Faculty of Engineering and Natural Sciences
Sabanci University
Orhanli, Tuzla
Istanbul
Turkey 34956
e-mail:ebudak@sabanciuniv.edu

Editorial Board

D. Ben-Arieh (USA)
C. Brecher (Germany)
H. van Brussel (Belgium)
B. Çatay (Turkey)
F. T. S. Chan (Hong Kong)
F. F. Chen (USA)
G. Chryssolouris (Greece)
C. K. Chua (Singapore)
M. Combacau (France)
A. Crosnier (France)
S. S. Dimov (UK)
L. Fratini (Italy)
M. W. Fu (Hong Kong)
H. Huang (Australia)
V. K. Jain (India)
M. K. Jeong (USA)
P. Ji (Hong Kong)
W.-Y. Jywe (Taiwan)
R. T. Kumara (USA)
A. Kusiak (USA)
B. Lauwers (Belgium)
W. B. Lee (Hong Kong)
C. R. Nagarajah (Australia)
E. Niemi (Finland)
D. T. Pham, (Book Review Editor, UK)
S. G. Ponnambalam (Malaysia)
M. M. Ratnam (Malaysia)
V. R. Rao (India)
C. Saygin (USA)
W. Steen (UK)
D. J. Stephenson (UK)
M. K. Tiwari (India)
E. Vezzetti (Italy)
G. Vosniakos (Greece)
X. Xu (New Zealand)
Y. X. Yao (China)
A. R. Yildiz (Turkey)
M. Zaeh (Germany)
H.-C. Zhang (USA)
L. Zhang (Australia)
A.G. Mamalis (Greece)

Founding Editor: Professor B. John Davies (1924-2013)

READ THIS JOURNAL ON SPRINGERLINK

Online First Articles

All Volumes & Issues

FOR AUTHORS AND EDITORS

2016 Impact Factor   **2.209**

Aims and Scope

Submit Online

Open Choice - Your Way to Open Access

Instructions for Authors

Call for Papers: Special Issue "Machinin...

SERVICES FOR THE JOURNAL

Contacts

Download Product Flyer

Shipping Dates

Order Back Issues

Article Reprints

Bulk Orders

ALERTS FOR THIS JOURNAL

Get the table of contents of every new issue published
in The International Journal of Advanced Manufacturing
Technology.

Your E-Mail Address

SUBMIT

☐ Please send me information on new Springer
publications in Industrial and Production Engineering.

ADDITIONAL INFORMATION

How to sign up for ToC alerts

RELATED BOOKS - SERIES - JOURNALS

Book

Handbook of
Manufacturing
Engineering and
Technology

Editor» Nee, Andrew Yeh Ching
(Ed.)

CrossMark

ORIGINAL ARTICLE

Investigation of the micro-milling process of thin-wall features of aluminum alloy 1100

D.L. Zariatin[1] · G. Kiswanto[1] · T.J. Ko[2]

Abstract Thin-wall geometrical features are observed in many mechanical components, including micro-components such as blades of a micro-impeller and the walls of a micro-channel. Although several papers have already presented research studies regarding thin-wall development, there is still a lack of information regarding how thin a wall could be produced via micro-milling processes. This paper investigates thin-wall quality in terms of the shape and dimension, the problems faced by micro-milling technology in producing thin-wall features, and the feasibility of producing thin-wall components using a micro-milling process aluminum alloy 1100 (AA110). The minimum wall thickness of 11.71 μm was successfully machined in good condition. The actual deviation of the wall thickness, including the tool dimension incompatibility, was in the range of −4.69 to 3.48 μm. A 16-blade micro-impeller with average blade thickness of 11.96 μm was manufactured. Among the 16 blades, four cloven blades, nine deflected blades, and three blades were in good condition.

✉ G. Kiswanto
gandjar_kiswanto@eng.ui.ac.id

[1] Department of Mechanical Engineering, Universitas Indonesia, Depok, Indonesia

[2] School of Mechanical Engineering, Yeungnam University, Gyeongsan, Republic of Korea

1 Introduction

The word "thin-wall" is relative to the unit and its application. In micro-channel application, a thin-wall is defined as a wall with less than 100 μm of thickness and with an aspect ratio greater than 5 [1]. Thin-wall is a basic shape of mechanical components such as pipe, blades of an impeller or turbine, wall of a micro-channel, and fin of a heat exchanger. There are many aspects that must be considered to manufacture a thin-wall product using a micro-milling machine, such as accuracy of the machine tools [2, 3], thermal stability of the machine tools [4], vibration of the machine tool [5] and workpiece [6, 7], rigidity of the machine tools [8], tools and workpiece [9], deflection of the tools [10] and workpiece [11], and the cutting force [12, 13].

1.1 Literature review on micro-milling of thin-wall features

There are several research studies that involved successful manufacturing of thin-walls. Li et al. [14] successfully manufactured various thicknesses of thin-walls. The wall thickness was designed at 6, 8, 10, 12, 15, 20, 30, and 50 μm. The machining results showed that design thickness of 8 μm was successfully produced with 10 μm of actual thickness and an aspect ratio of 50. Thin-walls were manufactured using a new toolpath strategy. The proposed toolpath was validated by experiments. In the experiments, the thin-wall feature workpieces made of AISI H11 with 54 HRC and Böhler M261 with 46 HRC were machined on commercial KERN Evo machine tools using 0.5-mm diameter TiAln-coated ultra-fine grain tungsten carbide.

Annoni et al. [15] investigated the effects of wall thickness (10, 30, 50, and 70 μm), milling strategy (up-milling and down-milling), and toolpath selection (water line and step

support toolpath) on the wall quality and the cutting forces. A thin-wall feature with 10 μm of thickness on 0.4% carbon steel material was successfully manufactured by using Sandvik CoroMill Plura R216.12-02030-BS30P cutting tools, with a 2-mm cutting diameter. The machining process was performed using KERN Evo machine tools. The research result indicated that down-milling is more critical for the geometrical error (total flatness deviation and the average thickness error) of the thin-wall compared to the up-milling strategy. The toolpath factor does not affect the geometrical responses viability; however, application of the step support toolpath and the use of up-milling strategy were recommended.

Popov et al. [16] stated that there are two important issues in producing thin features: (1) the machining strategy selection taking into account the specific geometry of the component (including the selection of the cutting depth) and (2) the selection of the spindle speed and the feed-rate, which depends on the workpiece, the cutting tool materials, the tool geometry, and the chosen strategy. In their research, thin features with a design thickness of 20 μm were produced. The machining was performed by using a KERN HSPC 2216 micromachining center. Two hundred-micrometer and 150-μm DIXI 7242R flat ends were used to cut brass. Two variations of the spindle speed and the feed-rate used in the machining process were 39,000 RPM and 70 mm/min, respectively, and 40,000 RPM and 65 mm/min, respectively. Meanwhile, the step depth and stepover were 0.005 and 0.070 mm, respectively. Three machining processes with different strategies were performed. It is found that the proposed machining strategy was the most appropriate for milling thin features. The machining step should be performed with sufficiently low spindle speed to prevent any vibration during the machining process.

Another investigation regarding the thin-wall feature was performed by Agirre [17]. The wall was designed with thicknesses of 25, 50, and 75 μm. The machining process for the brass workpiece material was performed by using a developed four-axis micro-end milling machine. Three-level variations of the toolpath strategy, axial depth of cut, and feed per tooth were applied. The observation during the machining process concluded that some failures on 25-μm thin-wall thickness were caused from a large piece of entry and exit burrs.

On the other hand, Llanos [18] investigated the effects of machining strategies to optimize the final quality of the thin-walls in terms of straightness of the machined thin-walls, uniformity of wall thickness, and burr presence. The research found that a down-milling cutting direction with a Z-step milling strategy at a spindle speed of 35,000 RPM, an axial depth of cut of 150 μm, and a feed-rate of 150 mm/min produced the best overall thin-wall quality for brass (CuZn36Pb3). A down-milling cutting direction with a ramp milling strategy, a spindle speed of 25,000 RPM, an axial depth of cut of 150 μm,
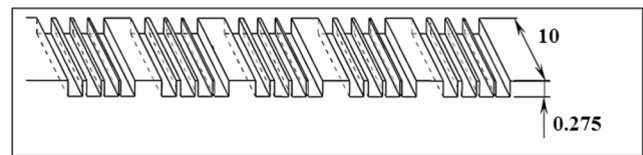

Fig. 1 The design of the thin-wall features (unit in mm)

and a feed-rate of 200 mm/min produced the best quality for aluminum (Al6061-T4). Another paper of Thepsonthi and Özel [19] also investigated the optimized cutting parameter and machining strategy to produce the best quality of Ti-6Al-4V titanium alloy. The research found that feed-rate was the major process parameter affecting the surface roughness. Higher feed-rate provides a better surface roughness and channel quality [20].

Although there are many researchers that investigated the quality of thin-wall products, there is still a lack of information regarding the minimum thickness that can be produced, especially by a miniaturized micro-milling machine, the problems in producing thin-walls, and the effect of the cutting parameters on the thin-wall quality. In this research, an investigation regarding the thin-wall quality in terms of the shape and dimensions, the problems faced by micro-milling technology in producing the thin-wall feature, and the feasibility of producing thin-wall components using a micro-milling process were performed.

2 Experimental setup

In this study, the thin-wall features were designed as an array on a rectangular workpiece 10,000 μm in length and 275 μm in height, as shown in Fig. 1. The wall thickness was designed to vary as 70, 50, 30, 20, 15, 10, 8, 5, and 3 μm, with the designed aspect ratios of 3.93, 5.5, 9.16, 13.75, 18.33, 27.55, 34.375, and 55. Two flutes of carbide flat-end-mill TiAln-coated tools with diameter of 200 μm were used to machine the AA1100 workpiece material. To ensure the quality of the tools, the actual geometries and dimension of the tools were inspected using SEM.

The combination of feed-rate, spindle speed, and machining strategy was designed as detailed in Table 1. Two levels of

Table 1 Combination of feed-rate, spindle speed, and machining strategy

Run	Feed-rate (Vf, mm/min)	Feed per tooth (fz, mm)	Spindle speed (n, RPM)	Machining strategy
1	30	0.00021	70,000	Zig
2	30	0.00016	95,000	Follow contour
3	60	0.00043	70,000	Follow contour
4	60	0.00032	95,000	Zig

Depth per cut = 10 μm

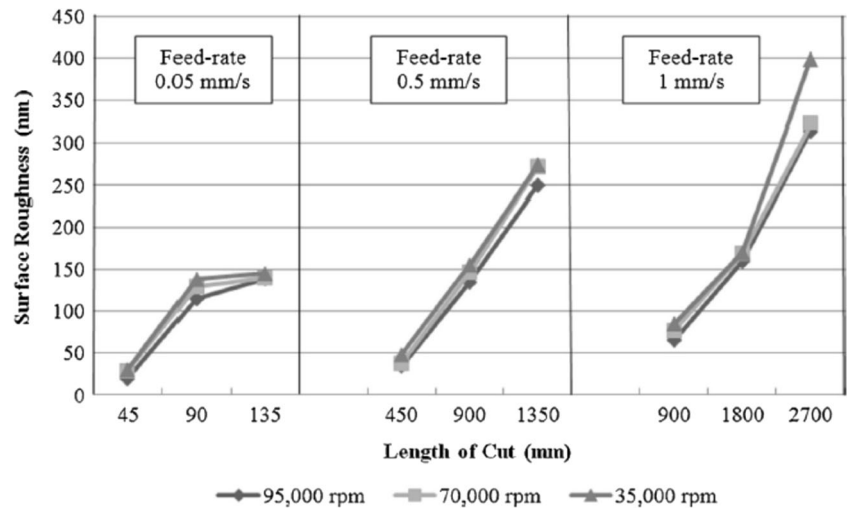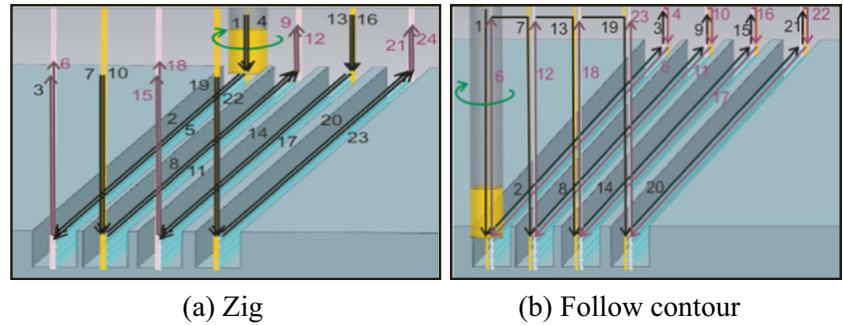Fig. 2 Predicted value of the surface roughness [21]

Fig. 3 Machining strategy. **a** Zig. **b** Follow contour
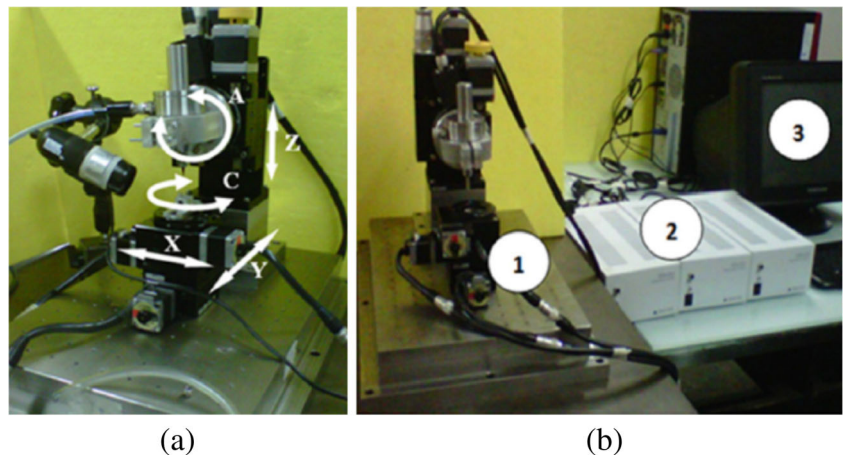

(a) Zig (b) Follow contour

feed-rate, spindle speed, and machining strategy were selected based on previous research [21]. To manufacture three series of thin-walls with different thicknesses on a workpiece 10,000 μm in length and 275 μm in height required a length of cut of 2200 mm. By selecting a depth of cut of 10 μm, 28 layers and 8 steps were required for each side of cutting. Figure 2 shows the prediction of the surface roughness of approximately 300 nm up to 400 nm of the machining process on AA1100 with a depth per cut of 10 μm, spindle speeds of

70,000 and 95,000 RPM, and feed-rates of 30 and 60 mm/min to produce a length of cut of 2200 mm.

There are several types of machining strategies: zig, zig-zag, follow contour, and follow profile. However, zig, follow contour, and follow profile are the machining strategies that can be considered to maintain the up-milling cutting direction. Zig is a one-way cutting direction and was selected to perform the up-milling cutting direction, as shown in Fig. 3a. Run 1 and run 4 as listed in Table 1 were used as zig cutting strategies.

Fig. 4 Miniaturized micro-milling machine used in the experiments. **a** Axis direction of XYZAC. **b** Micro-milling machine (*1*), DS102/112 (*2*), PC (*3*)

(a) (b)

Meanwhile, the follow contour toolpath strategy is a cutting direction that follows the part contour, as shown in Fig. 3b. Run 3 and run 2 as listed in Table 1 were used as follow contour cutting strategies. The difference between the zig and follow contour machining strategies was the cutting sequence.

In this research, the experiments were performed using a miniaturized five-axis micro-scale milling machine, as shown in Fig. 4. The linear axis (X, Y, Z) and rotational axis (A, B) are moved by Suruga Seiki motor steppers. Figure 4b shows the micro-milling machine components which consist of micro-milling machine construction (labeled by number 1), a DS102/112 controller that controls the motor stepper for each axis movement (labeled by number 2), and a PC to interpret the 3D model of impeller into a CL file (labeled by number 3). The linear accuracy of the machine tool was inspected using a Renishaw ML10 laser interferometer with two different cycles: unidirectional and bidirectional movement. The measurement revealed that the linear accuracy for the X, Y, and Z axes are 4.172, 1.263, and 4.352 µm, respectively.

An air turbine spindle HTS1501S-M2040 was used to rotate the cutting tools. The spindle accuracy is within its tolerance, according to the product specification.
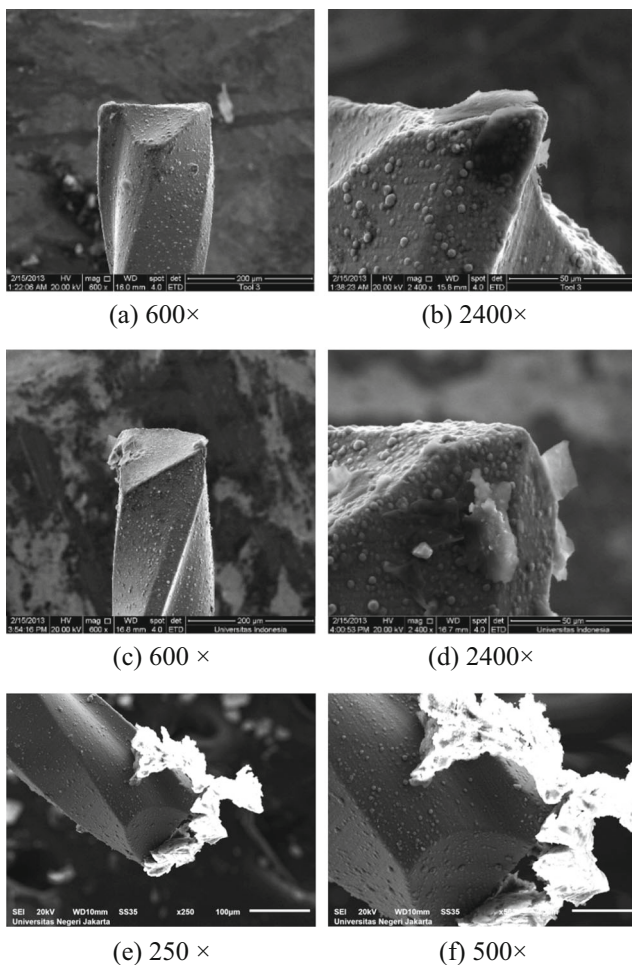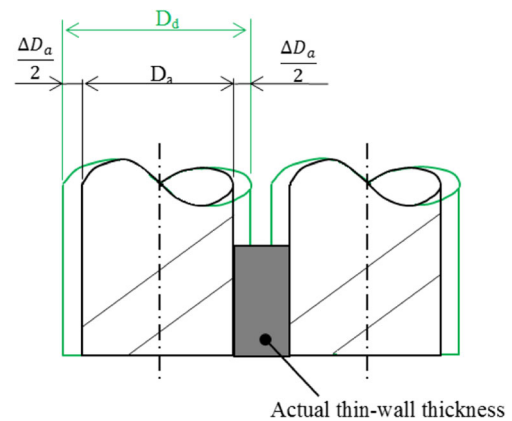

Fig. 6 Deviation of the tool diameter

2.1 Tool inspection

The tool plays an important role in the cutting process. Therefore, it is necessary to inspect the tool condition before beginning the machining process. Due to the small size of the tools used in the micro-milling process, the tool inspection must be performed using a scanning electron microscope (SEM); however, in many cases using a digital microscope with adequate magnification is sufficient.

The tool inspection revealed that the actual tool diameters were not precisely the same as the value in the tool specification. Furthermore, certain tools were not in good condition. A new tool must have a sharp and clean cutting edge; however, Fig. 5 shows several cases of rejected cutting tools delivered by the manufacturer. The tools were supposed to be rejected, instead of being delivered to customers.

The actual tool diameter (D_a, µm) measured in this research was primarily less than 200 µm (D_d). This difference would affect the wall thickness because the toolpath was designed with 200 µm tool diameter, as illustrated in Fig. 6. The
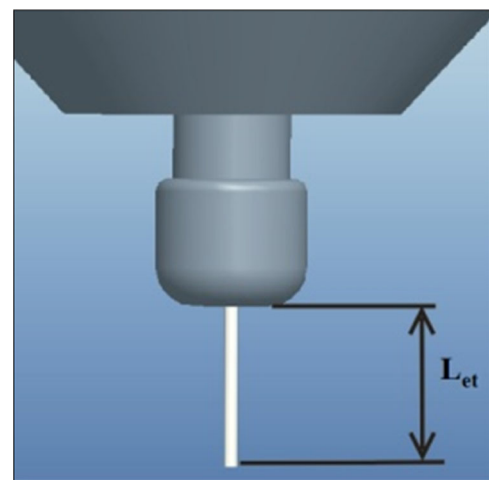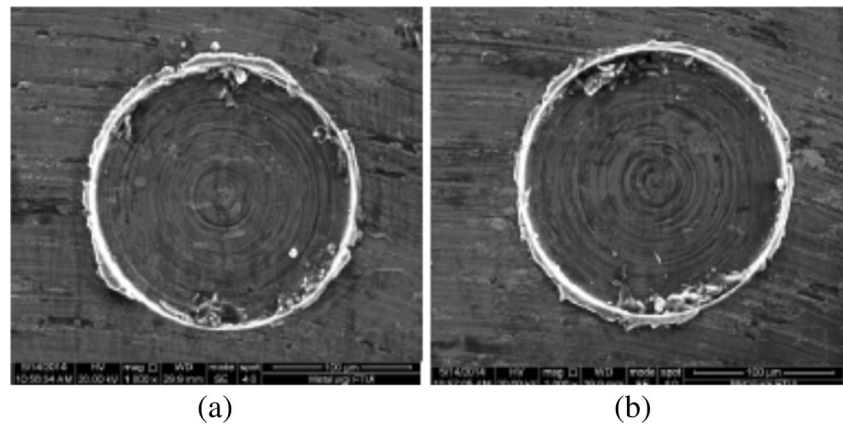

(a) 600×   (b) 2400×

(c) 600 ×   (d) 2400×

(e) 250 ×   (f) 500×

Fig. 5 Condition of rejected 200-µm diameter tools

Fig. 7 The tool length from the collets to the tool tip (L_{et})

Fig. 8 The circular pocket of the actual tool run-out test for a tool with actual diameter of 186 μm, L_{et} of 7.26 mm, and spindle speed of **a** 95,000 RPM and **b** 70,000 RPM

(a)   (b)

deviation of the actual and designed tool diameter is expressed as ΔD_a (μm), as follows:

$$\Delta D_{ad} = D_d - \Delta D_a \quad (1)$$

The actual wall thickness (T_a, μm) produced by the machining process was not always the same as the designed thickness (T_d, μm). The thickness deviation is caused by many factors that influence the accuracy of machining process. The deviation (ΔT_{da}, μm) between the actual wall thickness and the designed wall thickness was calculated by using Eq. (2). Meanwhile, the thickness deviation by considering tool diameter deviation (ΔT_{ae}, μm) was calculated by using Eq. (3).
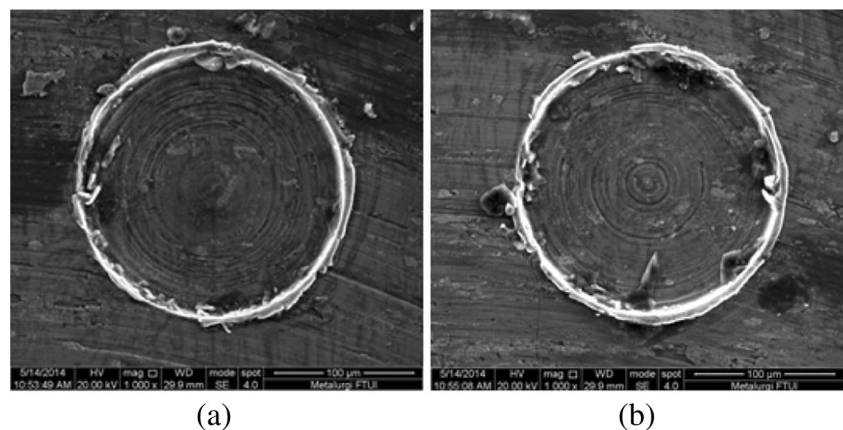
$$\Delta T_{da} = T_a - T_d \quad (2)$$
$$\Delta T_{ae} = T_a - T_d - \Delta D_a \quad (3)$$

2.2 Tool run-out measurement

Before performing the machining process, the actual tool run-out must be investigated because it affects the thin-wall dimension. A plunge milling with a 10-μm depth of cut was conducted to produce a circular pocket. The actual tool run-out was measured by comparing the differences between the actual tool

diameter and the circular pocket diameter. There are several parameters that must be considered in investigating the actual run-out, such as tool characteristics (e.g., material, shape, and dimension), workpiece characteristics (e.g., hardness, toughness, rigidity, ductility), and cutting parameters (e.g., spindle speed, cutting force, vibration). However, in this research, only two parameters were considered, as depicted in Fig. 7: the spindle speed and the length between the collets to the tooltip (L_{et}).

Figure 8 shows the circular pockets created by a 186-μm diameter tool with L_{et} of 7.26 mm that is rotated at 95,000 and 70,000 RPM. Meanwhile, Fig. 9 shows the circular pockets of a 187-μm diameter tool with L_{et} of 6.26 mm. The actual tool run-out, the difference between the tool diameter, and the circular pocket diameter are calculated for each case, as presented in Table 2. The results show that the higher values of the spindle speed and L_{et} caused a greater run-out error.

3 Micro-milling of channels with thin-walls

3.1 Thin-wall thickness measurement

Figure 10 shows thin-wall features that were designed with thicknesses of 70, 50, and 30 μm for each combination of feed-rate, spindle speed, and machining strategy. Figure 11

Fig. 9 The circular pocket of the actual tool run-out test for a tool with actual diameter of 187 μm, L_{et} of 6.26 mm, and spindle speed of **a** 95,000 RPM and **b** 70,000 RPM

(a)   (b)

Table 2 Actual tool run-out

| Tool actual diameter = 186 μm and L_{et} = 7.26 mm			
n = 95,000 RPM		n = 70,000 RPM	
Pocket diameter	Run-out	Pocket diameter	Run-out
194.33 μm	8.33 μm	193.91 μm	7.91 μm
Tool actual diameter = 187 μm and L_{et} = 6.26 mm			
n = 95,000 RPM		n = 70,000 RPM	
Pocket diameter	Run-out	Pocket diameter	Run-out
192.44 μm	5.44 μm	191.39 μm	4.39 μm

shows thin-wall features that were designed with thicknesses of 20, 15, and 10 μm. Meanwhile, Fig. 12 shows thin-wall features that were designed with thicknesses of 8, 5, and 3 μm. However, the actual thickness of each thin-wall was eventually different from the designed thickness.

The actual wall thicknesses produced in this research were determined by measuring the wall thickness using SEM pictures, as listed in Table 3. The table shows that the minimum thin-wall thickness produced in this research is 11.71 μm. The cutting parameter used in the zig machining strategy was a spindle speed of 95,000 RPM and a feed-rate of 60 mm/min.
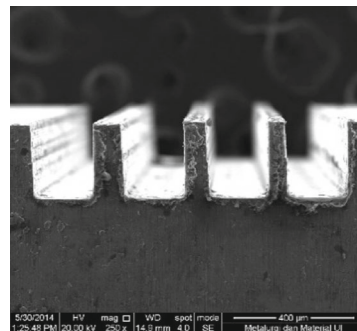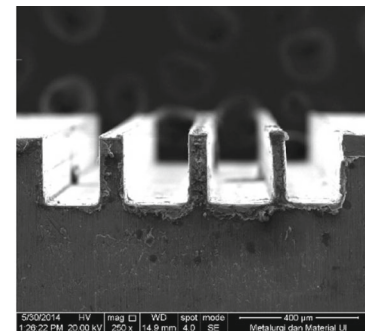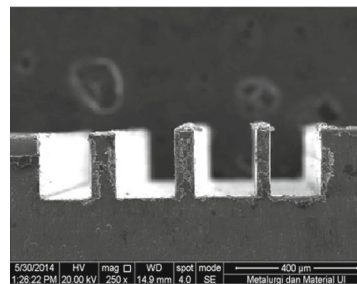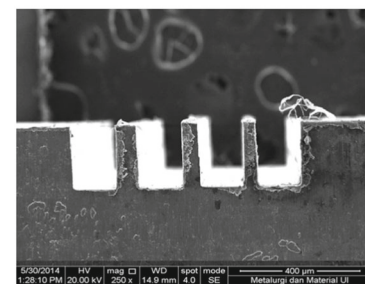
Figure 12d shows that the wall thickness of 11.71 μm is in good condition. However, a deflection occurs on the thin-wall with 16.70 μm thickness. The wall length is 10,000 μm, so there is a possibility of deflection of the thin-wall. The material characteristic selection (considering rigidity and stiffness), product handling, and cleaning after the machining process are very important to maintain to avoid the thin-wall deflection.

3.2 Effect of micro-milling parameters

The relationship of the feed-rate (f, mm/min) and the spindle speed (n, RPM) to the wall thickness deviation, ΔT_{da} and ΔT_{ae}, are shown in Figs. 13 and 14. However, the analysis was performed based on ΔT_{ae} because ΔT_{ae} already neglects the tool dimension deviation.

Figure 14a, b shows that the spindle speed of 95,000 RPM produced smaller ΔT_{de} compared to the spindle speed of 70,000 RPM for each feed-rate of 30 and 60 mm/min. Normally, the tool run-out diminishes the wall thickness. The tool provides a negative value to the wall thickness. However, due to other errors that occur during the cutting process, the tool run-out apparently improved the wall thickness deviation. However, the spindle speed of 95,000 RPM has an irregular tendency to achieve the design thickness for each feed-rate,

Fig. 10 Thin-wall features that were designed with thicknesses of 70, 50, and 30 μm, for each combination of feed-rate (Vf, mm/min), spindle speed (n, RPM), and machining strategy
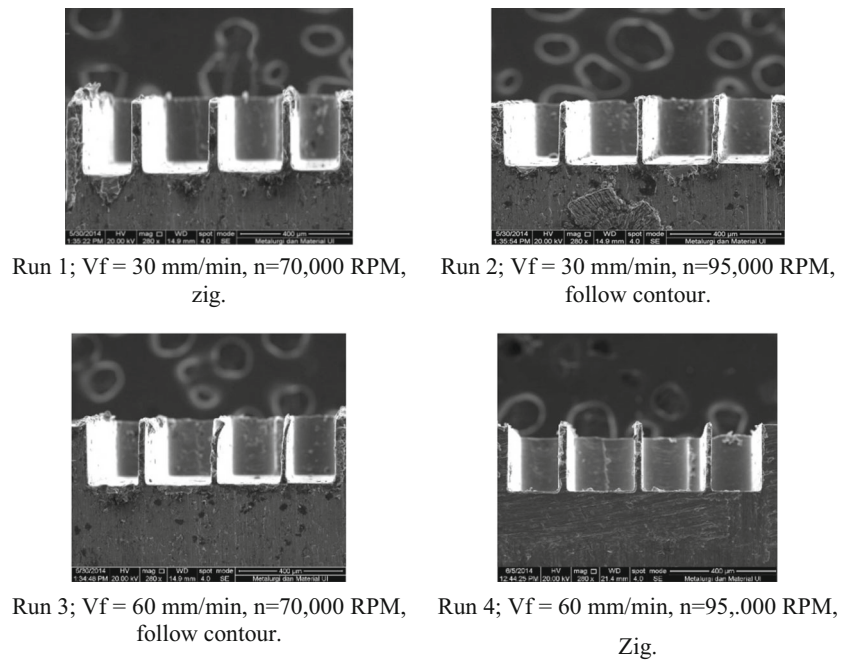

Run 1; Vf = 30 mm/min, n=70,000 RPM, zig.

Run 2; Vf = 30 mm/min, n=95,000 RPM, follow contour.

Run 3; Vf = 60 mm/min, n=70,000 RPM, follow contour.

Run 4; Vf = 60 mm/min, n=95,000 RPM,

Zig.

Fig. 11 Thin-wall features that were designed with thicknesses of 20, 15, and 10 μm, for each combination of feed-rate (*Vf*, mm/min), spindle speed (*n*, RPM), and machining strategy

Run 1; Vf = 30 mm/min, n=70,000 RPM, zig.

Run 2; Vf = 30 mm/min, n=95,000 RPM, follow contour.

Run 3; Vf = 60 mm/min, n=70,000 RPM, follow contour.

Run 4; Vf = 60 mm/min, n=95,.000 RPM, Zig.

30 and 60 mm/min, as shown in Fig. 14. Therefore, if other errors in the machining process could be eliminated, the lower spindle speed would result in better accuracy of the wall thickness.

Based on the bottom surface roughness measurement of the thin-walls, it was found that the highest surface roughness value is 349 nm. The surface roughness value is in the range of surface prediction as shown in Fig. 2.

3.3 Tool wear analysis

According to ISO 8688-2:1989, tool life testing and criterion in the milling process is based on the average and localized flank wear to be 300 and 500 μm, respectively. However, this standard is inappropriate to evaluate the micro-tool life [19] and there is no standard that regulates the tool life criterion in the micro-milling process. In this research, the tool wear was

Fig. 12 Thin-wall features that were designed with thicknesses of 8, 5, and 3 μm, for each combination of feed-rate (*Vf*, mm/min), spindle speed (*n*, RPM), and machining strategy
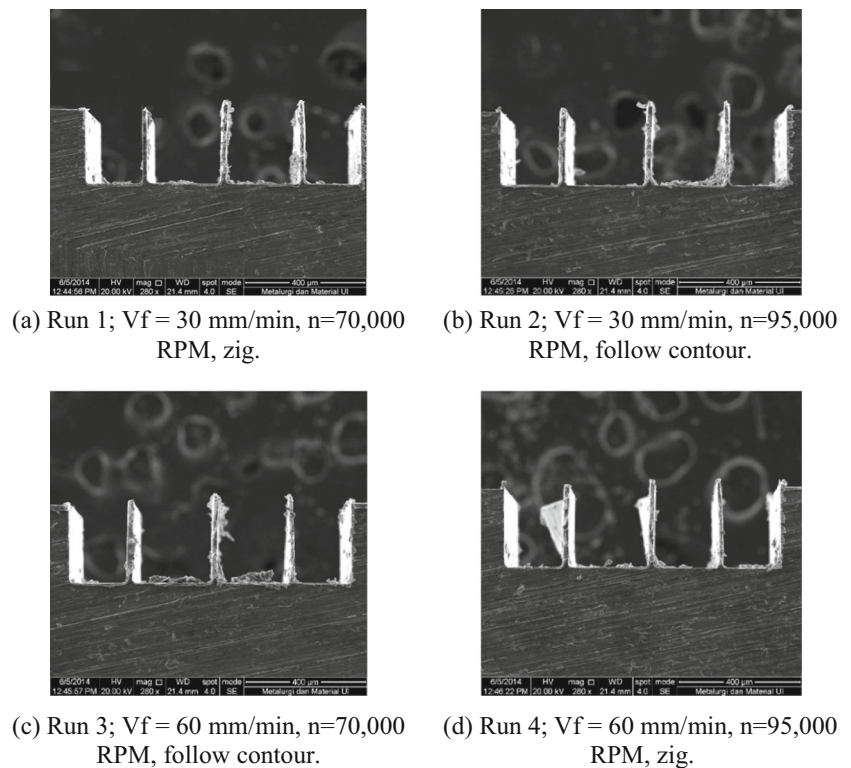

(a) Run 1; Vf = 30 mm/min, n=70,000 RPM, zig.

(b) Run 2; Vf = 30 mm/min, n=95,000 RPM, follow contour.

(c) Run 3; Vf = 60 mm/min, n=70,000 RPM, follow contour.

(d) Run 4; Vf = 60 mm/min, n=95,000 RPM, zig.

Table 3 Thin-wall thickness (T, μm)

T_d	Run 1 $Vf = 30$ mm/min, $n = 70,000$ RPM, zig			Run 2 $Vf = 30$ mm/min, $n = 95,000$ RPM, follow contour			Run 3 $Vf = 60$ mm/min, $n = 70,000$ RPM, follow contour			Run 4 $Vf = 60$ mm/min, $n = 95,000$ RPM, zig		
	T_a	ΔT_{da}	ΔT_{ae}	T_a	ΔT_{da}	ΔT_{ae}	T_a	ΔT_{da}	ΔT_{ae}	T_a	ΔT_{da}	ΔT_{ae}
	Tool diameter = 178 μm			Tool diameter = 186 μm			Tool diameter = 179 μm			Tool diameter = 184 μm		
70	95.48	25.48	3.48	80.72	10.72	−3.28	93.61	23.61	2.61	81.74	11.74	−4.26
50	75.16	25.16	3.16	60.13	10.13	−3.87	73.05	23.05	2.05	61.31	11.31	−4.69
30	55.39	25.39	3.39	40.64	10.64	−3.36	53.81	23.81	2.81	41.87	11.87	−4.13
	Tool diameter = 187 μm			Tool diameter = 193 μm			Tool diameter = 188 μm			Tool diameter = 191 μm		
20	29.41	9.41	−3.59	23.76	3.76	−3.24	28.31	8.31	−3.69	25.53	5.53	−3.47
15	24.17	9.17	−3.83	18.51	3.51	−3.49	22.84	7.84	−4.16	20.32	5.32	−3.68
10	19.44	9.44	−3.56	13.76	3.76	−3.24	18.87	8.87	−3.13	15.61	5.61	−3.39
	Tool diameter = 185 μm			Tool diameter = 187 μm			Tool diameter = 186 μm			Tool diameter = 188 μm		
8	18.48	10.48	−4.52	17.23	9.23	−3.77	17.98	9.98	−4.02	16.70	8.70	−3.30
5	15.48	10.48	−4.52	14.23	9.23	−3.77	14.48	9.48	−4.52	13.96	8.96	−3.04
3	13.73	10.73	−4.27	12.73	9.73	−3.27	12.48	9.48	−4.52	11.71	8.71	−3.29

Depth per cut = 10 μm

T_d designed thickness (μm), T_a actual thickness (μm), ΔT_{da} deviation between designed and actual thickness (μm, see Eq. (2)), ΔT_{ae} deviation of designed and actual thickness by calculating the tool diameter deviation (ΔD_a) (μm, see Eq. (3))

measured by using SEM. Figure 15 shows the condition of tools that is used in the machining process. The wear of the tool used with a spindle speed of 70,000 RPM and a feed-rate of 30 mm/min is 0.01 μm (Fig. 15a); the wear of the tool used with a spindle speed of 95,000 RPM and a feed-rate of 60 mm/min is 0.29 μm (Fig. 15b). The amount of wear that occurs

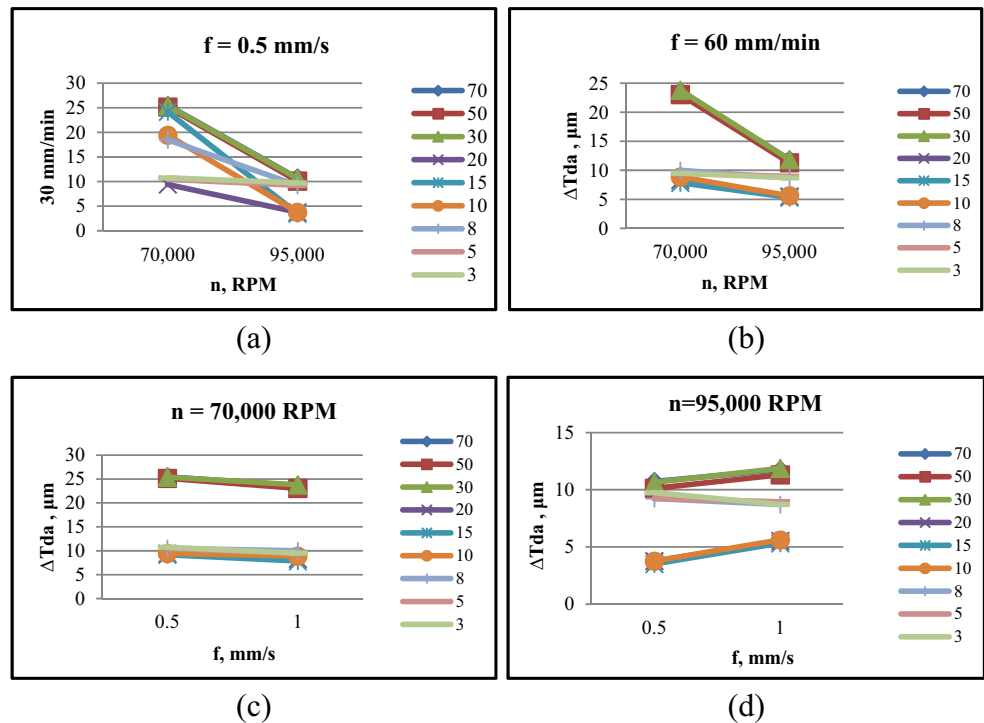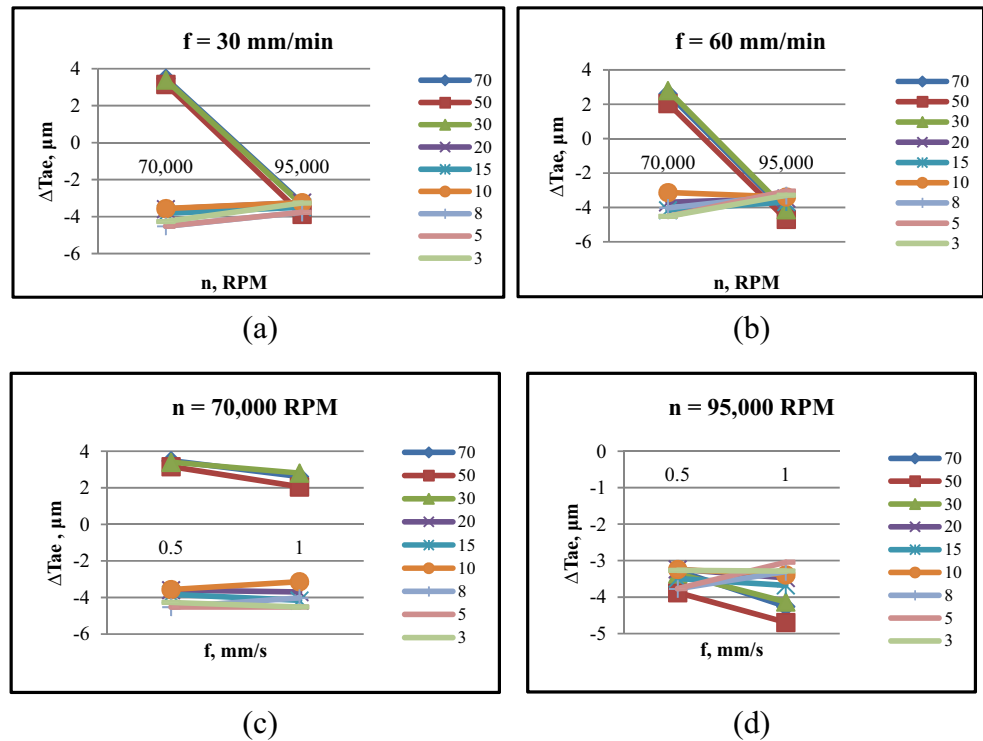**Fig. 13** The relation of ΔT_{da} for each feed-rate and spindle speed

(a)

(b)

(c)

(d)

Fig. 14 The relation of ΔT_{de} for each feed-rate and spindle speed

(a)

(b)

(c)

(d)

on both tools is less than the depth per cut selected for the machining process of 10 μm. Therefore, the tools are assumed to be in good condition, even after the cutting process.

4 Micro-milling of a micro-impeller with thin-blades

4.1 Micro-impeller design

A micro-impeller blade is a real example of a thin-wall feature on a component. To determine the capability of the micro-milling process in producing a micro-impeller, an aluminum alloy 1100 (AA1100) micro-impeller was
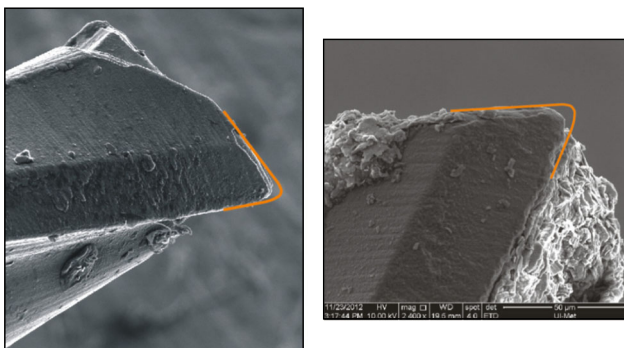
designed and manufactured. The 16-blade micro-impeller design was thin-walls with a thickness of 25 μm. The blade has a radius form within 1.7 mm. The micro-impeller design is shown in Fig. 16.

4.2 Micro-milling strategy and toolpath

A flat-end carbide TiAlN with diameter of 2 mm was used for facing and roughing process. Meanwhile, a flat-end carbide TiAlN-coated tool with actual diameter of 204.92 μm was used for semi-finishing and finishing processes. The tool was in a perfect condition, as shown in Fig. 17. The spindle speed, feed-rate, and depth per cut were 70,000 RPM, 30 mm/min, and 10 μm, respectively. Meanwhile, the depth of cut was different for each facing, roughing, semi-finishing and finishing process.
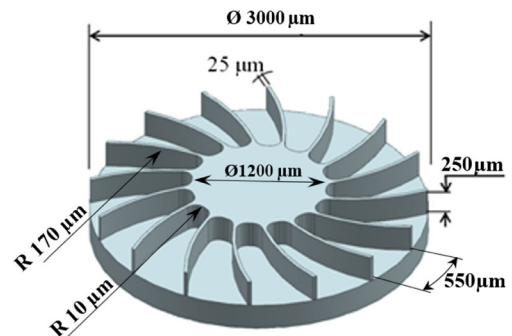

(a) Spindle speed of 70,000 RPM, feed-rate of 30 mm/min

(b) Spindle speed of 95,000 RPM, feed-rate of 60 mm/min

Fig. 15 Condition of the tools after the cutting process

Fig. 16 A micro-impeller design

Fig. 17 New tool condition before the machining process

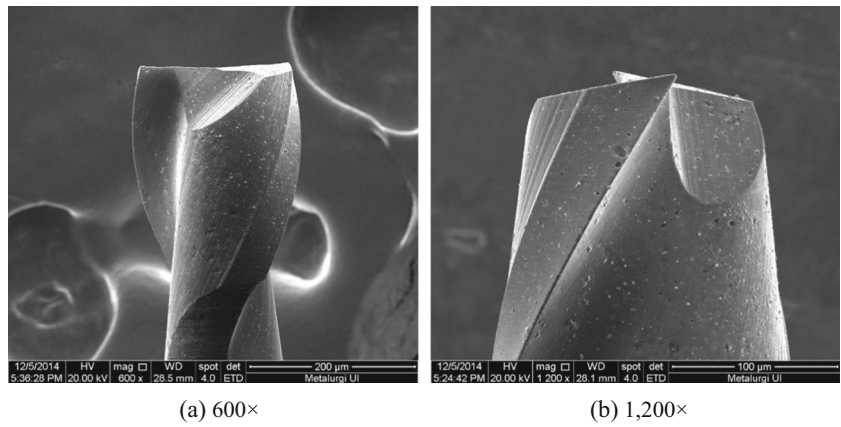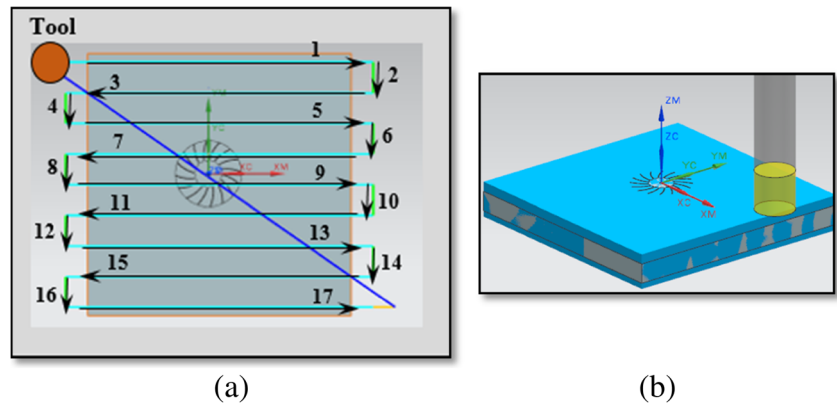(a) 600×

(b) 1,200×

Fig. 18 Facing process. **a** Toolpath. **b** Cutting simulation

(a)

(b)

zig-zag toolpath was used for the facing process. Figure 18 shows the toolpath for the facing process. The roughing and finishing processes are performed by using a *follow countor* toolpath, as shown in Fig. 19a, c, d, meanwhile the semi-

finishing process is performed by using a *zig-zag* toolpath as shown in Fig. 19b.

4.3 Thin-blade measurement

The machining result of the micro-impeller is shown in Fig. 20. Meanwhile, the detailed dimension of the product is listed in Table 4.

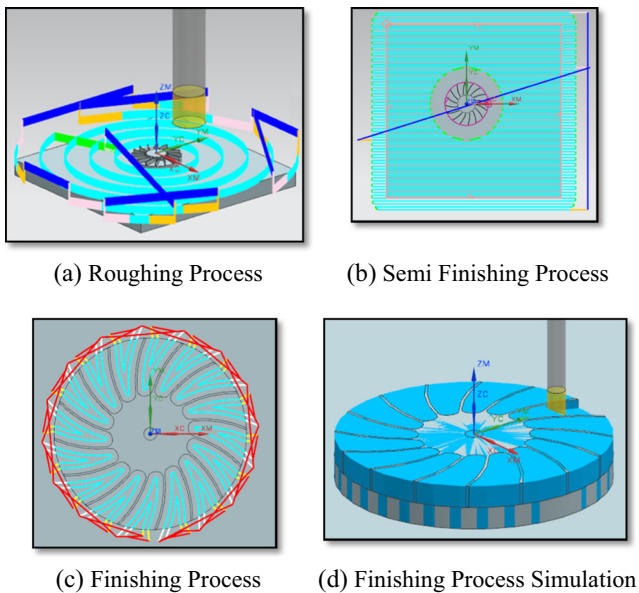Figure 21 shows that, among the 16 blades, there are four cloven blades and nine deflected blades, and only

(a) Roughing Process

(b) Semi Finishing Process

(c) Finishing Process

(d) Finishing Process Simulation

Fig. 19 Machining strategy. **a** Roughing process. **b** Semi-finishing process. **c** Finishing process. **d** Finishing process simulation
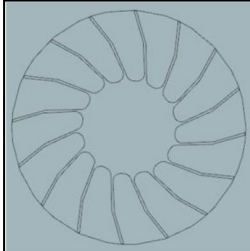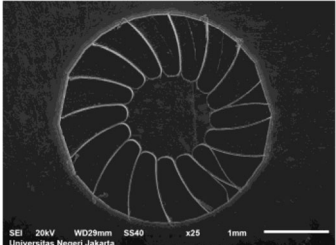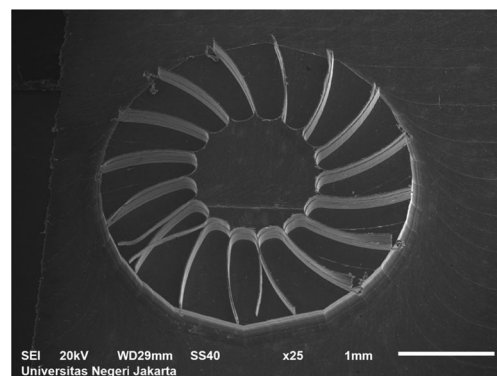

Fig. 20 Sixteen-blade micro-impeller with 11.96 μm average blade thickness

Table 4 Micro-impeller design and product information

No.	Parameters	Design (μm)	Product (μm)
1	Micro-impeller diameter	3.200	3.230
2	Outside distance between blades	552	610
3	Blade height	250	290
4	Impeller height	500	560
5	Average blade thickness	25	11.96
6	Shape conformity		

three blades are in good condition. Figure 21 shows the details of failure that occurs in the micro-impeller blade due to the thickness of the blade. Figure 21a, c shows a deflected blade with a small torn part on the edge of the blade (marked by a circle). The cloven apparently occurs after the blade had experienced deflection on the edge of the blade. The blade becomes cloven as it was torn to the inside direction.

Figure 22 shows the tool condition after 33 min of the cutting process. A visual observation of the tool shows that it was still in good shape. The wear of the tool is 0.64 μm, or approximately 6.4% in the range of the depth per cut.
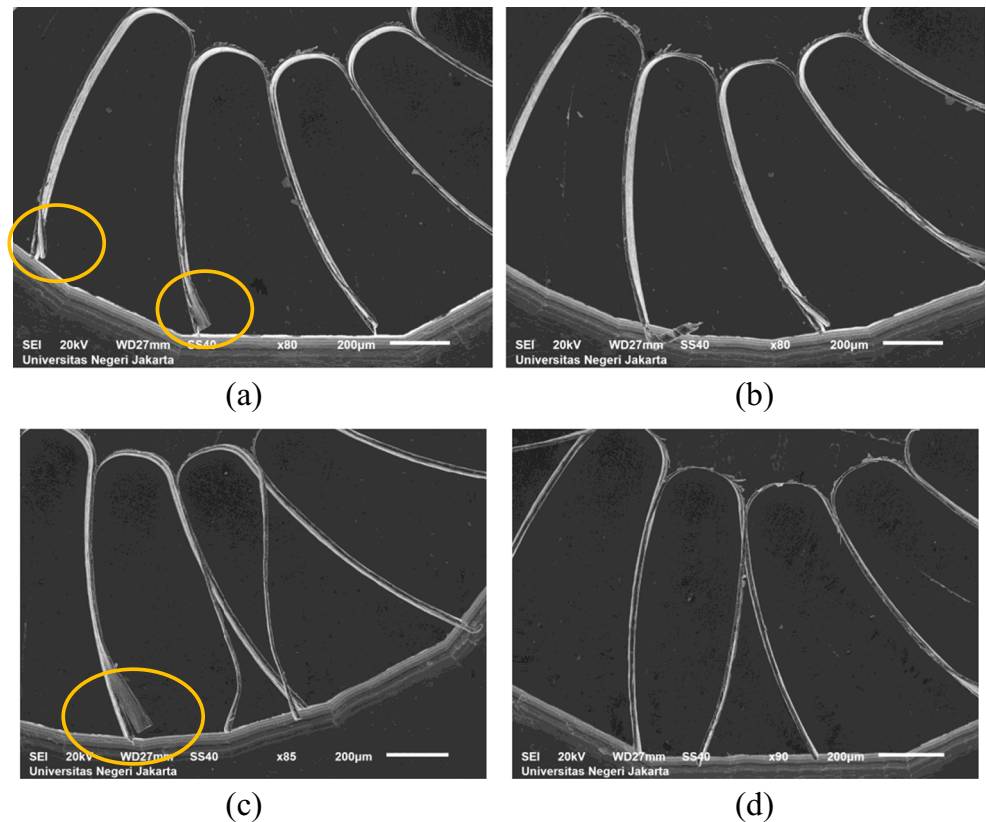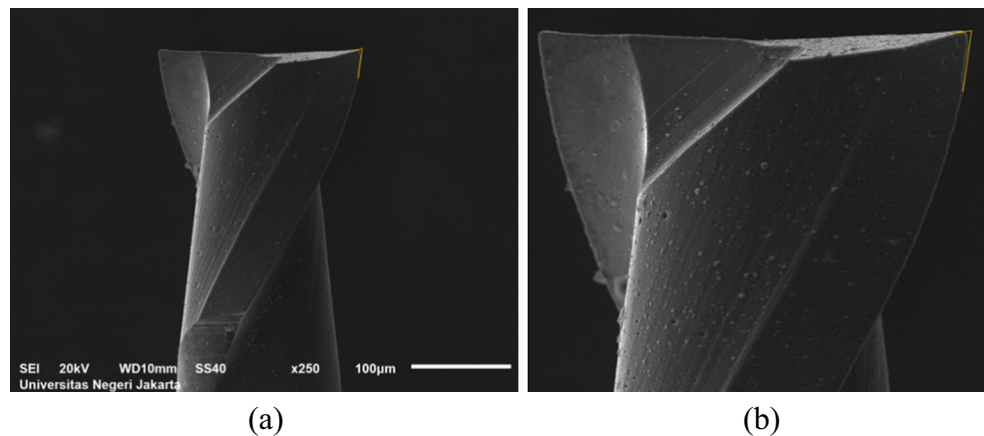
Fig. 21 The failure on the blades

(a)

(b)

(c)

(d)

Fig. 22 Tool condition after the machining process

(a)   (b)

Every material has its own characteristic, property, and specific threshold, as well as AA1100. Deflections of the micro-impeller blades probably occurred due to the wall thickness exceeding the material threshold of rigidity and strength. Apparently, a wall thickness less than 12 μm has the possibility of deflection. The material threshold is influenced by many factors, such as the cutting force, run-out, rigidity, stiffness, and vibration, whereas the accumulation of one factor or more influences the material threshold.

5 Conclusions

Before performing a machining process, it is important to inspect the tool dimensions and condition because there is possibility that the tool dimension is not the same as that in the specification. Moreover, sometimes the tools are not in perfect shape and condition. It is also important to check the actual tool run-out because it provides information about the actual deviation that occurs for a specific material, tool, and machine. There are many factors that affect the actual tool run-out, such as the tool positioning and spindle speed selection. The smallest length between the collets to the tooltip (L_{et}) and the proper spindle speed would minimize the actual tool run-out.

Based on the machining process performed in this research, it is found that the minimum thickness of the thin-wall feature was 11.71 μm. The wall was designed to have a thickness of 3 μm. However, due to the deviation of the tool diameter, the design thickness was actually 15 μm. Therefore, the deviation of the actual thickness by neglecting the deviation of the tool diameter is −3.29 μm.

The deviation of the actual wall thickness produced by a miniaturized micro-milling machine is in the range of −4.69 to 3.48 μm. There was no specific correlation found among spindle speed, feed-rate, and machining strategy with the thin-wall accuracy. Handling and cleaning after the machining process

must be performed with care because it might cause deflection of the wall.

A 16-blade micro-impeller was manufactured as an example of thin-wall features. The average blade thickness was 11.96 μm. Among the 16 blades, there were four cloven blades, nine deflected blades, and only three blades in good condition. Apparently, the cloven occurs after the blade had experienced deflection on the edge of the blade. Blade becomes cloven as it was torn towards the inside direction. Apparently, a wall of thickness less than 12 μm has the possibility to deflect.

References

1. Yarin L, Musyak A, Hetsroni G (2009) Fluid flow, heat transfer and boiling in micro-channels. Springer, Heidelberg
2. Huo D, Cheng K, Wardle F (2010) Design of five-axis ultra-precision micro-milling machine—UltraMil part 1: holistic design approach, design consideration and spesification. International Journal Advance Manufacturing Technology 47(9–12):867–877
3. Huo D, Chneg K, Wardle K (2010) Design of five-axis ultra-precision micro-milling machine—UltraMill. Part 2 : integrated dynamic, modeling, design optimization and analysis. International Journal Advance Manufacturing Technology 47(9–12):879–890
4. Creighton E, Honegger A, Tulsian A, Mukhopadhyay A (2010) Analysis of thermal errors in a high-speed micro-milling spindle. International Journal of Machine Tools & Manufacture 50:386–393
5. Fortgang JD 2006 Combined mechanical and command design for micro-milling machines, Georgia
6. Weinert K, Kersting P, Surmann T, Biermann (2008) Modeling regenerative workpiece vibration in five-axis milling. Prod Eng 2(3):255–260
7. Seguy S, Dessein G, Arnaud L (2008) Surface roughness variation of thin wall milling, related to modal interaction. International Journal of Machine Tools & Manufacture 48(3–4):261–274
8. Luo X, Cheng K, Webb D, Wardle F (2005) Design of ultraprecision machine tools with application to manufacture of miniature and micro components. J Mater Process Technol 167(2–3):515–528

9. Wan M, Zhang W, Qui K, Gao T (July 2005) Numerical prediction of static form errors in peripheral milling of thin-walled workpieces with irregular meshes. J Manuf Sci Eng 127:13–22

10. Mamedov A, Layegh K SE and Lazoglu I (2013) Machining force and tool deflections in micro-milling. In: 14th CIRP Conference on Modeling of Machining Operation (CIRP CMMO)

11. Malekian M, Park SS, Jun MB (2009) Tool wear monitoring of micro-milling operations. J Mater Process Technol 209:4903–4914

12. Otieno A and Mirman C (2008) Finite element analysis of cutting forces and temperatures on microtools in the micromachining of aluminum alloys. In: Proceedings of The 2008 IAJC-IJME International Conference

13. Malekian M, Park SS, Jun MB (2009) Modeling of dynamic micro-milling cutting forces. International Journal of Machine Tools & Manufacture 49:586–598

14. Li P, Zdebski D, Langen HH, Hoogstrate AM, Oosterling JAJ, Schmid RHM, Allen DM (2010) Micromilling of thin ribs with high aspect ratios. J Micromech Microeng 20:115013 **(10pp)**

15. Annoni M, Rebaioli L and Semeraro Q (2015) Thin wall geometrical quality improvement in micromilling. Int J Adv Manuf Technol

16. Popov K, Dimov S, Pham D, Ivanov A (2006) Micromilling strategies for machining thin features. Proceeding of the Institution of Mechanical Engineering Part C : Journal of Mechanical Engineering Science 220(11):1):1677–1684

17. Agirre A, Thepsonti T, Tugrul O (2012) "Micro-milling of metalic thin-wall features with application in micro-heat sinks," in Ninth International Conference on HIGH SPEED MACHINING, San Sebastián

18. Llanos I, Agirre A, Urreta H, Thepsonthi T, Özel T (2014) Micromilling high aspect ratio features using tungsten carbide tools. Proceeding of the Institution Mechanical Engineering Part B, Journal of Engineering Manufacture 228:1350–1358

19. Thepsonthi T, Özel T (2014) An integrated toolpath and process parameter optimization for high-performance micro-milling process of Ti-6Al-4V titanium allo. Int J Adv Manuf Technol 75:57–75

20. Thepsonthi T, Özel T (2012) Multi-objective process optimization for micro-end milling of Ti-6Al-4V titanium alloy. Int J Adv Manuf Technol 63(9):903–914

21. Kiswanto G, Zariatin D, Ko T (June 2014) The effect of spindle speed, feed-rate and machining time to the surface roughness and burr formation of Aluminum Alloy 1100 in micro-milling operation. J Manuf Process 16:435–450